

Spin signature of nonlocal-correlation binding in metal organic frameworks

T. Thonhauser,^{1,*} S. Zuluaga,¹ C. A. Arter,¹ K. Berland,^{2,3} E. Schröder,² and P. Hyldgaard²

¹*Department of Physics, Wake Forest University, Winston-Salem, NC 27106, USA.*

²*Microtechnology and Nanoscience, MC2, Chalmers University of Technology, SE-412 96 Göteborg, Sweden.*

³*Centre for Materials Science and Nanotechnology (SMN), University of Oslo, 0316 Oslo, Norway.*
(Dated: September 15, 2015)

We develop a proper nonempirical spin-density formalism for the van der Waals density functional (vdW-DF) method. We show that this generalization, termed svdW-DF, is firmly rooted in the single-particle nature of exchange and we test it on a range of spin systems. We investigate in detail the role of spin in the nonlocal-correlation driven adsorption of H₂ and CO₂ in the linear magnets Mn-MOF74, Fe-MOF74, Co-MOF74, and Ni-MOF74. In all cases, we find that spin plays a significant role during the adsorption process despite the general weakness of the molecular-magnetic responses. The case of CO₂ adsorption in Ni-MOF74 is particularly interesting, as the inclusion of spin effects results in an increased attraction, opposite to what the diamagnetic nature of CO₂ would suggest. We explain this counter-intuitive result, tracking the behavior to a coincidental hybridization of the O *p* states with the Ni *d* states in the down-spin channel. More generally, by providing insight on nonlocal correlation in concert with spin effects, our nonempirical svdW-DF method opens the door for a deeper understanding of weak nonlocal magnetic interactions.

PACS numbers: 71.15.Mb, 31.15.ej, 81.05.Rm

The modular building-block nature of metal organic frameworks (MOFs) and their extraordinary affinity for adsorption of small molecules make these nano-porous materials ideal for technologically important applications. MOFs are used, for example, for gas storage and sequestration [1–5], catalysis [6, 7], polymerization [8, 9], luminescence [10, 11], non-linear optics [12], magnetic networks [13], targeted drug delivery [14], multiferroics [15–17], and sensing [18–21]. The design of novel MOFs with improved properties requires insight into the molecule/MOF interaction. The large unit cells and periodic nature of MOFs make density functional theory (DFT) the prospective tool for a theory exploration. However, both the adsorbate molecule and the MOF’s metal centers can carry spin, giving rise to complex magnetic interactions and a molecular-spin response. It is thus crucial that DFT can reliably capture van der Waals (vdW) forces—which govern adsorption in MOFs—in concert with spin effects.

Concerning the former, the last decade witnessed the development of DFT descriptions for these forces [22]. Here, the vdW-DF versions [23–26] stand out by being nonempirical exchange-correlation functionals that are systematic and truly nonlocal extensions beyond LDA [27] and GGA [28] in the electron-gas tradition [22, 29, 30]. Subsequent developments include variants which differ by their choice of the semi-local exchange [31–35] and related nonlocal correlation functionals that rely on optimizing parameters [36–38]. The vdW-DF method and relatives have been successfully applied to numerous materials in general [22, 29, 39], and to small-molecule adsorption in MOFs in particular [4, 5, 40–46].

Concerning the spin effects, however, a systematic description within the vdW-DF framework is still missing. Such effects can play important roles not only in MOFs,

but in many systems, as Hund’s rules reflect a preference for spin-polarized ground states. For example, spin and vdW effects are essential in organic spintronics [47], dimer binding in excited states [48], overlayer formation on magnetic substrates [49], and correctly assessing formation energies [50]. While the nonlocal functional VV09 considers spin in its own way [51, 52], there have so far only been pragmatic approaches for vdW-DF—ignoring the effect of spin on the nonlocal correlation altogether [53] or estimating the effect [54–56] using the semi-local correlation of PBE [28].

In this letter, we formulate a proper extension of vdW-DF to spin-polarized systems, termed svdW-DF, following the design-logic of the original functional. We apply svdW-DF to study the nonlocal-correlation driven adsorption of H₂ and CO₂ in MOF74 and find that spin plays a significant role, providing a detailed analysis of spin signatures in such vdW bonding. Beyond MOFs, we envision that svdW-DF will lead to wider materials-theory progress in a stimulating role like that of LSDA, i.e., LDA’s spin extension [27]. LSDA was introduced to describe bulk-cohesive and molecular-binding energies [50, 57, 58] but also led DFT to important successes in the study of magnetism [59]. The svdW-DF formulation enables a robust exploration of systems where spin and nonlocal correlations are both important and it makes vdW-DF a general purpose method [60].

To design svdW-DF as the natural extension of vdW-DF to spin-polarized systems, we revisit the derivation of its nonlocal correlation energy functional. The starting point is the adiabatic-connection formula (ACF) expressed in terms of a scalar dielectric function ϵ that reflects a formal average of the coupling-constant integration over the screened density-response function [23, 57, 61, 62]. This provides a split-up of the total exchange-

correlation energy into a nonlocal and semi-local piece $E_{xc}^{\text{vdW-DF}} = E_c^{\text{nl}} + E_{xc}^{\text{int}}$, defined by [22, 23, 25, 30] in terms of the Coulomb Green's function G and an integral over the imaginary frequency u :

$$E_c^{\text{nl}}[n] = \int_0^\infty \frac{du}{2\pi} \text{Tr} [\ln(\nabla\epsilon \cdot \nabla G) - \ln\epsilon] \quad (1)$$

$$E_{xc}^{\text{int}}[n] = \int_0^\infty \frac{du}{2\pi} \text{Tr} \ln\epsilon - E_{\text{self}}. \quad (2)$$

The general-geometry vdW-DF versions [23, 25, 26] expand the nonlocal correlation energy (1) in terms of a semi-local response function $S \equiv \ln\epsilon$ that is parameterized via the choice of internal semi-local (GGA-type) functional E_{xc}^{int} (2).

To obtain a computationally tractable approximation for E_c^{nl} [22, 23, 25], vdW-DF relies on a plasmon-pole approximation of S defined in plane-wave representation as $S_{\mathbf{q},\mathbf{q}'} = \frac{1}{2}\bar{S}_{\mathbf{q},\mathbf{q}'} + \frac{1}{2}\bar{S}_{-\mathbf{q}',-\mathbf{q}}$, with

$$\bar{S}_{\mathbf{q},\mathbf{q}'} = \int d\mathbf{r} e^{-i(\mathbf{q}-\mathbf{q}')\cdot\mathbf{r}} \frac{4\pi e^2 n(\mathbf{r})/m}{[\omega_q(\mathbf{r}) + \omega][\omega_{q'}(\mathbf{r}) - \omega]}. \quad (3)$$

Here, $n(\mathbf{r})$ is the total electron density and $\omega_q(\mathbf{r})$ is the effective local plasmon dispersion, parameterized by an effective response parameter in the form of an inverse length scale $q_0(\mathbf{r}) = q_0[n] = q_0(n(\mathbf{r}), \nabla n(\mathbf{r}))$; m and e are the electronic mass and charge. The link between the energy-per-particle of the internal functional $\varepsilon_{xc}^{\text{int}}(\mathbf{r})$ and $\omega_q(\mathbf{r})$ [22, 23, 30] follows from combining Eqs. (2) and (3) together with a plasmon dispersion $\omega_q(\mathbf{r}) = q^2/2h(q/q_0(\mathbf{r}))$ with a Gaussian shape of $h(x) = 1 - \exp(-\gamma x^2)$, where γ is an arbitrary constant set to $4\pi/9$. Expanding Eq. (1) to second order in S , one arrives at the well-known six-dimensional integral over a universal kernel $\Phi_0(a, b)$,

$$E_c^{\text{nl}} = \frac{1}{2} \int d\mathbf{r} d\mathbf{r}' n(\mathbf{r}) \Phi_0(q_0(\mathbf{r})|\mathbf{r}-\mathbf{r}'|, q_0(\mathbf{r}')|\mathbf{r}-\mathbf{r}'|) n(\mathbf{r}'), \quad (4)$$

which defines the approximation for E_c^{nl} [23]. The total exchange-correlation energy $E_{xc}^{\text{vdW-DF}}$ also consists of the semi-local functional E_{xc}^{int} (2). This is in practice approximated as $E_{xc}^{\text{int}} \approx E_{xc}^0 = E_x^{\text{GGA}} + E_c^{\text{LDA}}$, based on a number of criteria [23, 25, 26, 31, 32, 35] and differing from the internal functional E_{xc}^{int} to varying degrees.

The extension of the semi-local part E_{xc}^0 to spin-polarized systems is straightforward. It is given by the exact spin scaling of exchange [63], i.e. $E_x[n_\uparrow, n_\downarrow] = E_x[2n_\uparrow]/2 + E_x[2n_\downarrow]/2$, and the well-established spin-dependence of the local correlation [27]. Here n_\uparrow and n_\downarrow denote the spin-density components. Crucially, by applying the very same criteria, we obtain a fully consistent extension of E_c^{nl} for the spin case.

The spin-scaling of exchange results in a spin-dependent semi-local response S in Eq. (3), with spin entering exclusively in the denominator through $\omega_q(\mathbf{r})$.

The numerator is given by the f -sum rule, specified as the classical plasmon frequency which depends only on the total electron density $n(\mathbf{r})$. The formulation of svdW-DF can therefore be based on an universal-kernel evaluation using the exact same function $\Phi_0(a, b)$ as in vdW-DF. Nevertheless, the form of the effective response parameter q_0 —which acts as scaling parameter in the arguments of Φ_0 —must be adjusted, $q_0[n] \rightarrow \tilde{q}_0[n_\uparrow, n_\downarrow]$, to reflect the explicit spin dependence of the plasmon dispersion.

Motivating our procedure for extending the original vdW-DF formulations to spin-polarized system is the interpretation of the vdW-DF nonlocal correlation energy as a formal summation of zero-point energy shifts [30, 64, 65]. The vdW-DF framework starts with a description of the semilocal exchange-correlation holes corresponding to the internal functional E_{xc}^{int} [22, 25, 29], using a plasmon model to characterize the associated response. The vdW-DF nonlocal correlation energy (1) is a rigorous summation of the plasmon-pole shifts that result when such holes couple electrostatically [30]. Spin clearly affects the GGA-type internal hole and our svdW-DF formalism represents a proper implementation of how such semilocal spin effects impact the summation of zero-point energy shifts in Eq. (1).

To establish the updated form of $\tilde{q}_0[n_\uparrow, n_\downarrow]$ it is instructive to first revisit how $q_0[n]$ is specified in the spin-neutral case, where it is given as scaling of the Fermi wave vector $k_F(\mathbf{r}) = (3\pi^2 n)^{1/3}$ as follows

$$q_0(\mathbf{r}) = \frac{\varepsilon_{xc}^{\text{int}}(\mathbf{r})}{\varepsilon_x^{\text{LDA}}(\mathbf{r})} k_F(\mathbf{r}) \equiv q_{0c}[n] + q_{0x}[n], \quad (5)$$

$$q_{0c}[n] = -\frac{4\pi}{3e^2} \varepsilon_c^{\text{LDA}}, \quad (6)$$

$$q_{0x}[n] = -\left(1 - \frac{Z_{ab}s^2}{9}\right) \frac{4\pi}{3e^2} \varepsilon_x^{\text{LDA}}. \quad (7)$$

Here $\varepsilon_x^{\text{LDA}} = -3e^2 k_F/4\pi$ and the exchange gradient corrections are expressed in terms of the scaled gradient $s = |\nabla n|/2k_F n$. These relations (5)–(7) can be directly adapted to the spin case. The correlation part $\tilde{q}_{0c}[n_\uparrow, n_\downarrow]$ is specified by the spin-dependent PW92 LDA correlation energy-per-particle $\varepsilon_c^{\text{LDA}}$ [27]. For the exchange part $\tilde{q}_{0x}[n_\uparrow, n_\downarrow]$, the spin scaling relation [63] gives the following form

$$\tilde{q}_{0x}[n_\uparrow, n_\downarrow] = \frac{n_\uparrow}{n_\uparrow + n_\downarrow} q_{0x}[2n_\uparrow] + \frac{n_\downarrow}{n_\uparrow + n_\downarrow} q_{0x}[2n_\downarrow]. \quad (8)$$

These equations fully specify the nonlocal correlation energy of svdW-DF. We make svdW-DF self-consistent, implemented in QUANTUM ESPRESSO [66], by computing the corresponding exchange-correlation potential [24]. Further details on the implementation and calculations are provided in the Supplemental Material.

We test svdW-DF on three cases of increasing complexity; results are summarized here and details are in the Supplemental Material. For our test cases we use

the implementations svdW-DF1 [23] and svdW-DF2 [25] (which are better suited for small molecules) as well as svdW-DF-cx [26] (which is better suited for larger, extended systems). We start with the Li-dimer in its triplet state $^3\Sigma$ —an ideal test case that critically balances vdW and spin effects. We find a dissociation energy of 53 meV for svdW-DF1 and 70 meV for svdW-DF-cx, the former in good agreement with the experimental value of 41 meV [72]; VV10 and PBE find 77 meV. A second case is given by atomization energies for molecules from the G1 set [73], where spin enters through magnetic molecular ground states and the isolated atoms. We find a mean absolute percentage error of 4.59% and 7.75% for svdW-DF1 and svdW-DF-cx; VV10 and PBE find 5.14% and 7.11%, respectively. For a third, extended-system test, we study the weak-chemisorption of graphene on Ni(111) [74–76], finding a binding separation for svdW-DF-cx of 2.12 Å, in excellent agreement with experiment (2.11 ± 0.07 Å [74]). In contrast, svdW-DF1 finds 3.76 Å, VV10 finds 3.37 Å, and PBE essentially does not bind—unlike svdW-DF-cx they all miss a significant chemical component to the binding.

Table I summarizes the main point of this letter: that svdW-DF provides insight on the nature of nonlocal spin effects in the adsorption of H_2 and CO_2 in the linear magnets Mn-MOF74, Fe-MOF74, Co-MOF74, and Ni-MOF74 [77]. The table reports raw svdW-DF binding energies ΔE , as well as values ΔE_{ZPE} corrected for zero-point vibrations of the adsorbates and binding enthalpies at room temperature ΔH_{298} . We note that the adhesion comes entirely from E_c^{nl} —without nonlocal correlations, CO_2 would not bind at all and H_2 would only bind with a binding energy of ~ 5 meV.

Overall, we find very good agreement with experiment, which we partly attribute to the “cx” version of svdW-DF; agreement with other vdW-DF calculations is also good [5]. In all cases we find that the inclusion of spin has an important effect on the binding. Note that the case of Mn is somewhat artificial and the “no spin” num-

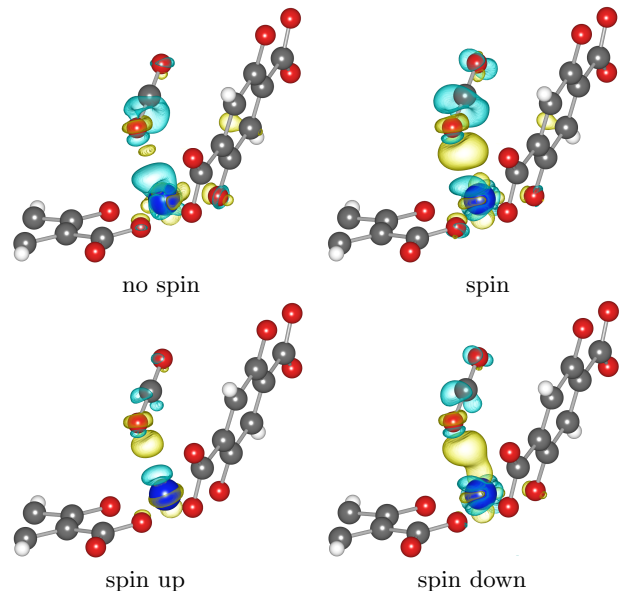


FIG. 1. (Upper panels) Induced charge density upon CO_2 adsorption in Ni-MOF74. (Lower panels) Induced charge density split into its up and down contribution. Blue (yellow) areas show charge depletion (accumulation). Iso levels are $0.001 e/\text{Bohr}^3$. See Fig. 3 in the Supplemental Material for the structure of the MOF.

bers seem inflated—this is a result of the fact that Mn-MOF74 itself requires spin for a proper description of its structure.

Of particular interest is the binding of CO_2 in Ni-MOF74, where spin effects play a tantalizing and unexpected role. The CO_2 molecule is diamagnetic and should experience a slight repulsion and weaker binding in the presence of the magnetic dipole of Ni—similarly to what is observed in all the other cases in Table I. However, on the contrary, when spin effects are included the binding increases and the molecule experiences a stronger attraction, which warrants further investigation. In the upper panels of Fig. 1 we plot the induced charge density, i.e., the charge density redistribution due to the formation of the bond. It is clearly visible that in the spin case more charge is pulled in-between the CO_2 and the metal site, resulting in the stronger binding. In the spin case, we can split this induced charge density further into spin-up and spin-down contributions, as shown in the lower panels of Fig. 1. Here we see the true spin effect: much more spin-down density is being pulled into the bond, compared to spin-up density. This peculiar behavior can be understood by analyzing the projected density of states in Fig. 2. In particular, from the middle and bottom panel we see that at -5 eV the O p states show similar peaks in the spin up and down channels. However, the projected Ni d states at that point have a large spin down density while the spin up density is much smaller. Thus, the O p states hybridize with the Ni spin-down d states,

TABLE I. Binding energies [meV] of small molecules in the system \mathcal{M} -MOF74+ \mathcal{A} with $\mathcal{M} = \text{Mn, Fe, Co, and Ni}$ and $\mathcal{A} = H_2$ and CO_2 . In number triplets the first number refers to the bare binding energy ΔE , the second one includes the zero-point correction ΔE_{ZPE} , and the third refers to the binding enthalpy at room temperature ΔH_{298} .

\mathcal{M}	\mathcal{A}	Exp.	no spin	spin
Mn	H_2	91 [67]	-473/-524/-524	-133/-117/-117
Fe	H_2	104 [68]	-134/-137/-137	-122/-124/-124
Co	H_2	111 [67]	-177/-181/-181	-111/-117/-117
Ni	H_2	134 [67]	-134/-137/-137	-131/-133/-133
Mn	CO_2	331 [69]	-528/-551/-550	-337/-345/-344
Fe	CO_2	352 [68]	-344/-353/-351	-315/-323/-321
Co	CO_2	383 [70]	-377/-387/-385	-350/-359/-357
Ni	CO_2	394 [71]	-300/-311/-309	-377/-390/-387

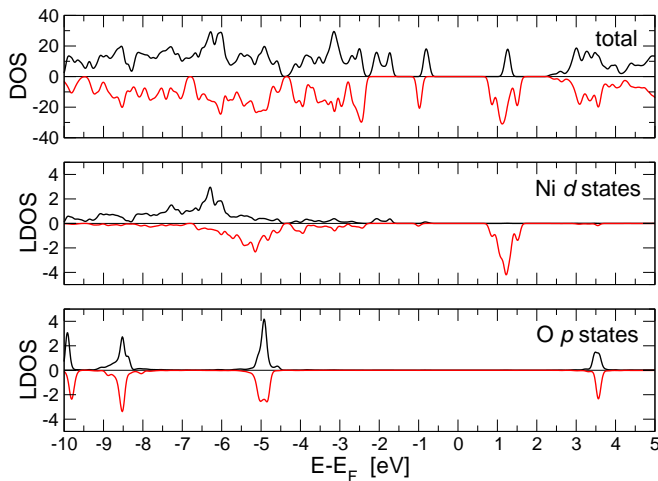


FIG. 2. Up (black) and down (red) total density of states (top) and projected density of states on the Ni d states (middle) and O p states (bottom) of the Ni-MOF74+CO₂ system.

while the hybridization with the spin-up states is negligible (see Fig. 4 in the Supplemental Material for plots of the corresponding orbitals). The interaction of the O p states with the down-spin Ni d states is therefore responsible for the increased and counter-intuitive strength of the bond.

As mentioned above, E_c^{nl} is responsible for the entire binding of the small molecules. As such, it is at least indirectly responsible for all the effects we see in our figures and tables. To examine the spin effect of E_c^{nl} explicitly, we also calculate the difference between the binding-induced density of a full svdW-DF calculation and the same calculation without the E_c^{nl} term (Fig. 5, Supplemental Material). Although overall smaller in magnitude—as expected, since the semi-local part E_{xc}^0 also contributes to the induced density—we find the same behavior as in Fig. 1: more down density is being pulled into the bond, strengthening the binding.

It is also revealing to partition the charge and magnetic moment of the system, as detailed in Table III in the Supplemental Material. Partitioning schemes are not unique, but one can still gain qualitative information. Before adsorption, the CO₂ has no magnetic moment and all six Ni atoms in the unitcell are equivalent. However, once adsorption occurs, the up and down charge inside the CO₂ rearranges differently and gives rise to a small but observable magnetic moment. At the same time, the adsorption process leaves the total charge on the CO₂ molecule unchanged, i.e. there is no net charge transfer. During this adsorption process, the nearby Ni loses 0.03 e —our analysis shows that it loses mostly down density—and thus its magnetic moment increases, giving rise to a weak nonlocal-correlation induced magnetic interaction.

Finally, in terms of absolute numbers, spin effects in the Fe-MOF74+CO₂ and Co-MOF74+CO₂ systems

seem to worsen agreement with experiment—but, at the same time, they actually resolve a more pressing issue. Experimentally, the CO₂ binding strength should follow the order Mn < Fe < Co < Ni. In calculations without spin (not considering the artificial case of Mn), the order is reversed. However, after including spin effects the correct order is restored.

In summary, we have developed a consistent spin-polarized version of the nonlocal exchange-correlation functional vdW-DF, which we find to now become an all-purpose functional. We then apply this framework to study small-molecule adsorption in MOF74 with magnetic open metal sites and find that including nonlocal spin effects can significantly influence the binding of the adsorbates. In the case of Ni-MOF-74+CO₂ we find a counter-intuitive increase in binding due to nonlocal spin effects, which we explain by a coincidental interaction of the Ni d and O p states. The additional degree of freedom from such unexpected magnetic interactions can be used to tailor the specificity of MOFs in novel gas storage, sequestration, and sensing applications.

Work in the US has been supported by NSF Grant No. DMR-1145968 and DOE Grant No. DE-FG02-08ER46491. Work in Sweden has been supported by grants from the Swedish Research Council (VR), the Swedish Foundation for Strategic Research (SSF), the Chalmers e-Science Centre, and the Chalmers Materials Area of Advance.

— Supplemental Material —

I. COMPUTATIONAL DETAILS

We have implemented svdW-DF in PWSCF 5.1, which is part of the QUANTUM ESPRESSO package [66]. We used ultrasoft pseudopotentials and a plane wave cutoff for the wave functions of 40 Ryd together with the cx [26] implementation of svdW-DF. Hubbard U corrections are applied to the d electrons of Mn, Fe, Co, and Ni, using the well-established values of 4.0, 4.0, 3.3, and 6.4 eV from Ref. [78], where the U values for each metal \mathcal{M} were determined so that they reproduce the experimental oxidation energy of the metal monoxide to $\mathcal{M}_2\text{O}_3$. Note that these U values have been shown to give highly accurate results for small-molecule adsorption in MOFs [5, 40]. Due to the large unitcell size of the MOF, we only sampled the Γ -point. In all our calculations, we optimized the entire structure until the forces on all atoms reached less than 1 meV/Å.

The starting points of the calculations are the experimental rhombohedral structures of Mn-, Fe-, Co-, and Ni-MOF74 with 54 atoms in the primitive cell. Table II shows the experimental lattice constants, listed in the more convenient hexagonal lattice [67, 79]. For the magnetic ordering of the metal ions we adopted the ferromagnetic arrangement, which has been found to be the ground-state configuration [77]. Figure 3 provides a graphical representation of the isostructural Mn-, Fe-, Co-, and Ni-MOF74.

Vibrational properties were calculated using the finite difference method with atomic displacements of 0.015 Å in each direction. The corresponding Hessian matrix was symmetrized and the acoustic sum rule was enforced. Only atoms of the adsorbed molecule were allowed to move—an approximation which we found to result in errors on the order of merely 1 cm⁻¹. The zero-point energy and the thermal correction to the binding energy was calculated as

$$\Delta E_{\text{ZPE}} + \Delta H_T = \frac{1}{2} \sum_i v_i + \sum_i \frac{v_i}{\exp(v_i/k_B T) - 1}, \quad (9)$$

where k_B is Boltzmann's constant and v_i are the vibrational frequencies of the system in eV. The temperature was set to $T = 298$ K. Contributions from low frequency vibrations were not included.

TABLE II. Experimental lattice constants used [Å] for our \mathcal{M} -MOF74 systems with $\mathcal{M} = \text{Mn, Fe, Co, and Ni}$.

\mathcal{M}	Ref.	$a = b$	c
Mn	[67]	26.230	7.035
Fe	[79]	26.098	6.851
Co	[67]	25.948	6.838
Ni	[67]	25.719	6.741

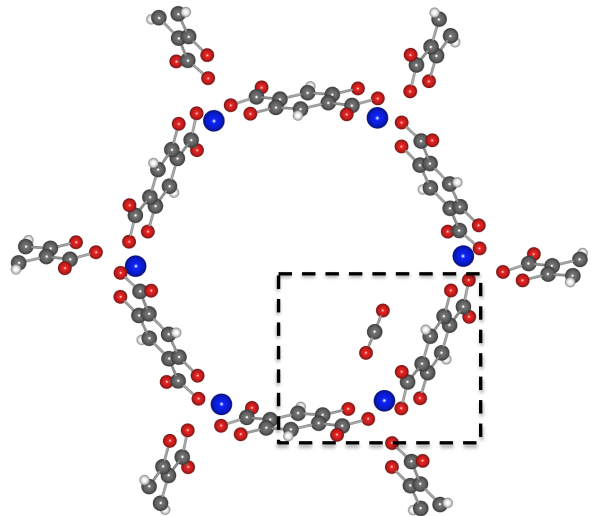


FIG. 3. MOF74 structure with a CO₂ molecule adsorbed at one of the open metal sites. The hexagonal channel structure with its six equivalent open metal sites per unit cell is clearly visible. Carbon atoms are depicted as grey spheres, while oxygen, hydrogen, and metal atoms are shown in red, white, and blue. The rectangle indicates the portion of MOF74 shown in the main manuscript and Figs. 4 and 5.

II. ADDITIONAL TABLES AND FIGURES

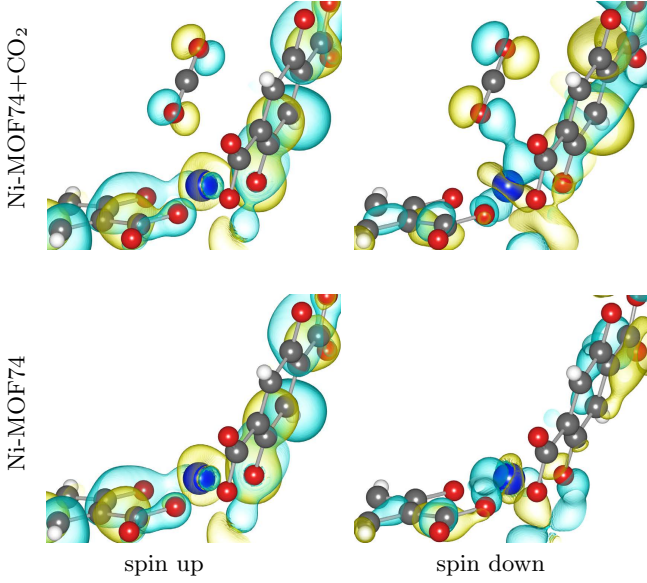


FIG. 4. Contour plots of $|\psi|^2 \times \text{sign}(\psi)$ evaluated (at the Γ -point) for the spin-up and spin-down Ni-MOF74 bands around -5 eV with (top row) and without (bottom row) the adsorbed CO_2 molecule. Iso levels are 0.0002 e/Bohr^3 . In all cases, the d_{z^2} -like orbital on the Ni is visible. In the spin-up channel, the adsorption of CO_2 leaves this orbital almost unchanged. In contrast, in the spin-down channel, the d_{z^2} -like orbital rotates towards the oxygen p orbital to form a new, hybridized orbital.

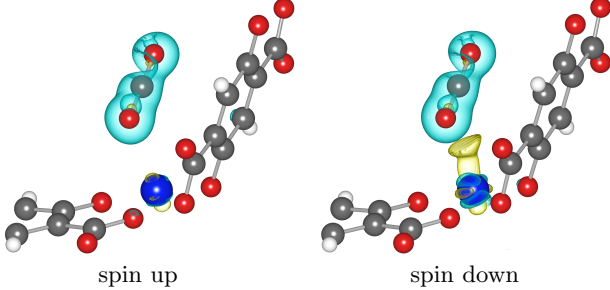


FIG. 5. Induced charge density originating from the E_c^{nl} term upon CO_2 adsorption Ni-MOF74, split into its up and down contribution. Blue (yellow) areas show charge depletion (accumulation). Iso levels are 0.0001 e/Bohr^3 .

TABLE III. Bader charge q (see Refs. [80, 81]) [in units of e , showing electron *loss* relative to the neutral unit] and magnetic moment μ [in units of μ_B] during the CO_2 adsorption process in Ni-MOF74. * indicates the Ni atom participating in the bond. Only one representative of the remaining 5 equivalent Ni is given.

Unit	before adsorption		after adsorption	
	q	μ	q	μ
CO_2	0.00	0.00	0.00	0.01
Ni*	1.30	1.57	1.33	1.60
Ni	1.30	1.57	1.30	1.57

III. SELF-CONSISTENT DERIVATIVES

As for the evaluation of $\tilde{q}_{0c}[n_\uparrow, n_\downarrow]$ and its derivatives, they are completely defined through the choice of correlation inside ϵ_c^{LDA} and are given elsewhere [27]. For $\tilde{q}_{0x}[n_\uparrow, n_\downarrow]$ it follows that

$$\frac{d\tilde{q}_{0x}[n_\uparrow, n_\downarrow]}{dn_\uparrow} = \frac{n_\downarrow}{(n_\uparrow + n_\downarrow)^2} (q_{0x}[2n_\uparrow] - q_{0x}[2n_\downarrow]) + \frac{2n_\uparrow}{n_\uparrow + n_\downarrow} \frac{dq_{0x}[n]}{dn} \Big|_{n=2n_\uparrow} \quad (10a)$$

$$\frac{d\tilde{q}_{0x}[n_\uparrow, n_\downarrow]}{dn_\downarrow} = \frac{n_\uparrow}{(n_\uparrow + n_\downarrow)^2} (q_{0x}[2n_\downarrow] - q_{0x}[2n_\uparrow]) + \frac{2n_\downarrow}{n_\uparrow + n_\downarrow} \frac{dq_{0x}[n]}{dn} \Big|_{n=2n_\downarrow} \quad (10b)$$

and

$$\frac{d\tilde{q}_{0x}[n_\uparrow, n_\downarrow]}{d|\nabla n_\uparrow|} = \frac{n_\uparrow}{n_\uparrow + n_\downarrow} \frac{dq_{0x}[2n_\uparrow]}{d|\nabla n_\uparrow|} \quad (11a)$$

$$\frac{d\tilde{q}_{0x}[n_\uparrow, n_\downarrow]}{d|\nabla n_\downarrow|} = \frac{n_\downarrow}{n_\uparrow + n_\downarrow} \frac{dq_{0x}[2n_\downarrow]}{d|\nabla n_\downarrow|}. \quad (11b)$$

IV. TESTING SVDW-DF

Testing and benchmarking has been performed on three model systems, i.e. the Li dimer in its triplet state $^3\Sigma$, atomization energies of a set of small molecules, and graphene on the Ni(111) surface. We used our implementation in PWSCF [66] and calculated binding curves and energies using svdW-DF1 [23], svdW-DF2 [25], svdW-DF-cx [26], VV10 [38, 82], and PBE [28]; these studies were performed using pseudopotentials from the Rutgers database with the recommended cutoffs [83]. Note that svdW-DF1 and svdW-DF2 are better suited for small molecules, while svdW-DF-cx is better suited for larger, extended systems. We compare our PWSCF calculations to high-level quantum chemistry (QC), diffusion Monte Carlo (DMC), and experiment where appropriate. Please see the footnotes [51] and [53] in the main text concerning the neglect of spin-polarization effects in the nonlocal part of VV10.

A. Li Dimer in the Triplet State $^3\Sigma$

TABLE IV. Dissociation energy D_e [meV] and fundamental frequency ω_e [meV] for Li_2 in the triplet state $^3\Sigma$. The experimental value is $D_e^{\text{exp}} = 41$ meV [72, 84]. Early papers using quantum chemistry methods report a considerable spread in D_e values [85–87], but the most recent high-level quantum chemistry (QC) results show in essence perfect agreement with experiment [48].

	svdW-DF1 [23]	svdW-DF2 [25]	svdW-DF-cx [26]	VV10 [38]	PBE [28]	QC [48]
D_e	53	55	70	77	77	41
ω_e	8	8	8	8	8	8

B. Atomization Energy of Small Molecules

TABLE V. Atomization energies E_{at} [eV] of small molecules from the G1 set [73]. Spin expectation values $\langle S(S+1) \rangle$ different from zero indicate a magnetic ground state. Diffusion Monte Carlo (DMC) values are taken from [88]; experimental numbers from [89]. An error analysis follows in Table VI. Spin enters through the isolated atoms and/or magnetic molecular ground states.

	$\langle S(S+1) \rangle$	svdW-DF1 [23]	svdW-DF2 [25]	svdW-DF-cx [26]	VV10 [38]	PBE [28]	DMC [88]	Exp. [89]
CH ₃	3/4	13.421	13.363	13.639	13.373	13.507	12.615	12.545
CH ₄	0	18.074	17.937	18.502	17.963	18.212	17.129	17.020
NH	2	3.763	3.810	3.758	3.795	3.778	3.393	3.426
NH ₂	3/4	7.942	7.934	8.100	7.957	8.042	7.339	7.372
NH ₃	0	12.648	12.516	13.088	12.620	12.880	11.991	11.999
OH	3/4	4.236	4.098	4.557	4.195	4.408	4.390	4.397
H ₂ O	0	9.660	9.449	10.194	9.612	9.953	9.514	9.512
SiH ₃	3/4	9.887	9.863	10.015	9.594	9.668	9.328	9.280
SiH ₄	0	13.921	13.941	14.086	13.528	13.595	13.261	13.122
PH ₂	3/4	6.716	6.694	6.899	6.572	6.656	6.232	6.275
H ₂ S	0	7.901	7.786	8.190	7.871	8.045	7.463	7.506
HCl	0	4.575	4.457	4.785	4.575	4.697	4.486	4.432
LiF	0	5.885	5.990	5.984	5.897	6.209	6.292	5.984
C ₂ H ₄	0	24.272	24.042	25.020	24.439	24.819	23.136	23.065
CO	0	10.940	10.732	11.489	11.179	11.501	10.981	11.110
N ₂	0	9.590	9.494	10.017	9.972	10.164	9.587	9.761
NO	3/4	6.373	6.133	7.043	6.725	7.079	6.198	6.507
O ₂	2	5.171	4.805	6.017	5.434	5.925	4.844	5.115
CO ₂	0	16.526	16.028	17.768	17.103	17.796	16.458	16.562
Na ₂	0	0.794	0.767	0.740	0.671	0.707	0.750	0.729
S ₂	2	4.820	4.650	5.197	5.161	5.334	4.264	4.365
NaCl	0	4.085	3.993	4.190	4.129	4.157	4.284	4.219
SiO	0	8.045	7.971	8.508	8.229	8.429	8.096	8.239
CS	0	7.504	7.374	7.861	7.801	7.980	7.172	7.328
SO	2	5.589	5.357	6.156	5.866	6.178	5.100	5.351

TABLE VI. Error analysis for the datasets given in Table V. Given are the mean (signed) percentage error (MPE), mean absolute percentage error (MAPE), and mean absolute deviation (MAD) values when comparing with experiment. Note that svdW-DF-cx, due to its design, is not necessarily expected to perform well for small molecules, but still gives good results, comparable to PBE.

	svdW-DF1 [23]	svdW-DF2 [25]	svdW-DF-cx [26]	VV10 [38]	PBE [28]	DMC [88]
MPE [%]	−3.28	−1.52	−7.69	−3.84	−6.75	0.54
MAPE [%]	4.59	4.50	7.75	5.14	7.11	1.65
MAD [eV]	0.37	0.38	0.67	0.40	0.59	0.11

C. Graphene on Ni(111)

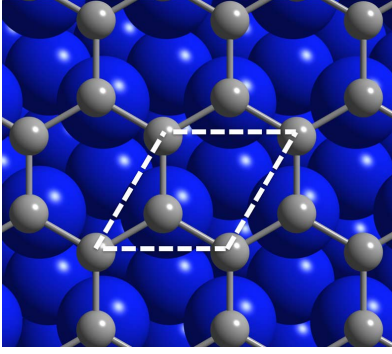


FIG. 6. Unit cell used for the adsorption of graphene on the Ni(111) surface. Ni was modeled as a slab consisting of 6 layers of atoms, the bottom three of which were fixed to their bulk positions. Blue and grey spheres denote Ni and C atoms, respectively.

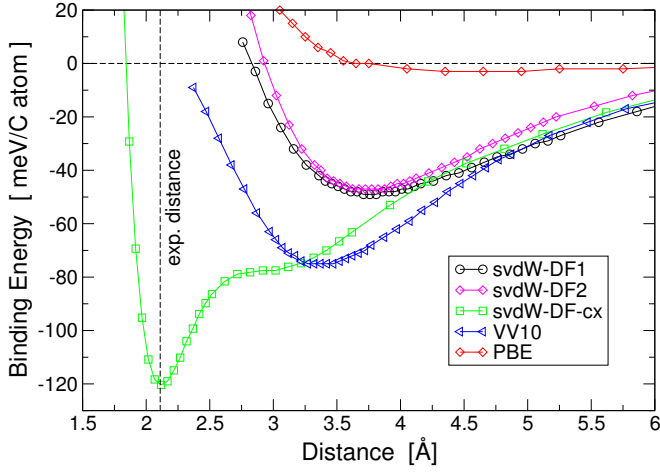


FIG. 7. Binding energy curve of graphene on the Ni(111) surface. The dashed vertical line denotes the experimental value for the distance between graphene and the Ni(111) surface [74].

* thonhauser@wfu.edu

- [1] L. J. Murray, M. Dinca, and J. R. Long, *Chem. Soc. Rev.* **38**, 1294 (2009).
- [2] J.-R. Li, Y. Ma, M. C. McCarthy, J. Sculley, J. Yu, H.-K. Jeong, P. B. Balbuena, and H.-C. Zhou, *Coord. Chem. Rev.* **255**, 1791 (2011).
- [3] S. Qiu and G. Zhu, *Coord. Chem. Rev.* **253**, 2891 (2009).
- [4] N. Nijem, H. Wu, P. Canepa, A. Marti, K. J. Balkus, T. Thonhauser, J. Li, and Y. J. Chabal, *J. Am. Chem. Soc.* **134**, 15201 (2012).
- [5] K. Lee, J. D. Howe, L.-C. Lin, B. Smit, and J. B. Neaton, *Chem. Mater.* **27**, 668 (2015).
- [6] J. Y. Lee, O. Farha, J. Roberts, K. A. Scheidt, S. T. Nguyen, and J. T. Hupp, *Chem. Soc. Rev.* **38**, 1450 (2009).
- [7] I. Luz, F. X. Llabrés i Xamena, and A. Corma, *J. Catal.* **276**, 134 (2010).
- [8] T. Uemura, N. Yanai, and S. Kitagawa, *Chem. Soc. Rev.* **38**, 1228 (2009).
- [9] M. J. Vitorino, T. Devic, M. Tromp, G. Férey, and M. Visseaux, *Macromol. Chem. Phys.* **210**, 1923 (2009).
- [10] M. D. Allendorf, C. A. Bauer, R. K. Bhakta, and R. Houk, *Chem. Soc. Rev.* **38**, 1330 (2009).
- [11] K. A. White, D. A. Chengelis, K. A. Gogick, J. Stehman, N. L. Rosi, and S. Petoud, *J. Am. Chem. Soc.* **131**, 18069 (2009).
- [12] S. Bordiga, C. Lamberti, G. Ricchiardi, L. Regli, F. Bonino, A. Damin, K.-P. Lillerud, M. Bjorgen, and A. Zecchina, *Chem. Commun.*, 2300 (2004).
- [13] M. Kurmoo, *Chem. Soc. Rev.* **38**, 1353 (2009).
- [14] P. Horcajada, T. Chalati, C. Serre, B. Gillet, C. Sebrie, T. Baati, J. Eubank, D. Heurtaux, P. Clayette, C. Kreuz, J.-S. Chang, Y. Hwang, V. Marsaud, P.-N. Bories, L. Cynober, S. Gil, G. Férey, P. Couvreur, and R. Gref, *Nat. Mater.* **9**, 172 (2010).
- [15] A. Stroppa, P. Jain, P. Barone, M. Marsman, J. M. Perez-Mato, A. K. Cheetham, H. W. Kroto, and S. Picozzi, *Angew. Chem., Int. Ed.* **50**, 5847 (2011).
- [16] A. Stroppa, P. Barone, P. Jain, J. M. Perez-Mato, and S. Picozzi, *Adv. Mater.* **25**, 2284 (2013).
- [17] D. Di Sante, A. Stroppa, P. Jain, and S. Picozzi, *J. Am. Chem. Soc.* **135**, 18126 (2013).
- [18] C. Serre, C. Mellot-Draznieks, S. Surblé, N. Audebrand, Y. Filinchuk, and G. Férey, *Science* **315**, 1828 (2007).
- [19] M. D. Allendorf, R. J. T. Houk, L. Andruskiewicz, A. A. Talin, J. Pikarsky, A. Choudhury, K. A. Gall, and P. J. Henske, *J. Am. Chem. Soc.* **130**, 14404 (2008).
- [20] J.-C. Tan and A. K. Cheetham, *Chem. Soc. Rev.* **40**, 1059 (2011).
- [21] L. Kreno, K. Leong, O. Farha, M. Allendorf, R. Van Duyne, and J. Hupp, *Chem. Rev.* **112**, 1105 (2012).
- [22] K. Berland, V. R. Cooper, K. Lee, E. Schröder, T. Thonhauser, P. Hyldgaard, and B. I. Lundqvist, *Rep. Prog. Phys.* **78**, 066501 (2015).
- [23] M. Dion, H. Rydberg, E. Schröder, D. C. Langreth, and B. I. Lundqvist, *Phys. Rev. Lett.* **92**, 246401 (2004).
- [24] T. Thonhauser, V. R. Cooper, S. Li, A. Puzder, P. Hyldgaard, and D. C. Langreth, *Phys. Rev. B* **76**, 125112 (2007).
- [25] K. Lee, E. D. Murray, L. Kong, B. I. Lundqvist, and D. C. Langreth, *Phys. Rev. B* **82**, 081101 (2010).
- [26] K. Berland and P. Hyldgaard, *Phys. Rev. B* **89**, 035412 (2014).
- [27] J. P. Perdew and Y. Wang, *Phys. Rev. B* **45**, 13244 (1992).
- [28] J. P. Perdew, K. Burke, and M. Ernzerhof, *Phys. Rev. Lett.* **77**, 3865 (1996).
- [29] K. Berland, C. A. Arter, V. R. Cooper, K. Lee, B. I. Lundqvist, E. Schröder, T. Thonhauser, and P. Hyldgaard, *J. Chem. Phys.* **140**, 18A539 (2014).
- [30] P. Hyldgaard, K. Berland, and E. Schröder, *Phys. Rev. B* **90**, 075148 (2014).
- [31] V. R. Cooper, *Phys. Rev. B* **81**, 161104 (2010).
- [32] J. Klimeš, D. R. Bowler, and A. Michaelides, *J. Phys. Condens. Matter* **22**, 022201 (2010).
- [33] J. Klimeš, D. R. Bowler, and A. Michaelides, *Phys. Rev. B* **83**, 195131 (2011).
- [34] J. Wellendorff, K. T. Lundgaard, A. Møgelhøj, V. Petzold, D. D. Landis, J. K. Nørskov, T. Bligaard, and K. W. Jacobsen, *Phys. Rev. B* **85**, 235149 (2012).
- [35] I. Hamada, *Phys. Rev. B* **89**, 121103 (2014).
- [36] O. A. Vydrov, Q. Wu, and T. Van Voorhis, *J. Chem. Phys.* **129**, 014106 (2008).
- [37] O. A. Vydrov and T. Van Voorhis, *Phys. Rev. Lett.* **103**, 063004 (2009).
- [38] O. A. Vydrov and T. Van Voorhis, *J. Chem. Phys.* **133**, 244103 (2010).
- [39] D. C. Langreth, B. I. Lundqvist, S. D. Chakarova-Käck, V. R. Cooper, M. Dion, P. Hyldgaard, A. Kelkkanen, J. Kleis, L. Kong, S. Li, P. G. Moses, E. D. Murray, A. Puzder, H. Rydberg, E. Schröder, and T. Thonhauser, *J. Phys. Condens. Matter* **21**, 084203 (2009).
- [40] R. Poloni, K. Lee, R. F. Berger, B. Smit, and J. B. Neaton, *J. Phys. Chem. Lett.* **5**, 861 (2014).
- [41] K. Lee, W. C. Isley, A. L. Dzubak, P. Verma, S. J. Stoneburner, L. C. Lin, J. D. Howe, E. D. Bloch, D. A. Reed, M. R. Hudson, C. M. Brown, J. R. Long, J. B. Neaton, B. Smit, C. J. Cramer, D. G. Truhlar, and L. Gagliardi, *J. Am. Chem. Soc.* **136**, 698 (2014).
- [42] P. Canepa, N. Nijem, Y. J. Chabal, and T. Thonhauser, *Phys. Rev. Lett.* **110**, 026102 (2013).
- [43] P. Canepa, C. A. Arter, E. M. Conwill, D. H. Johnson, B. A. Shoemaker, K. Z. Soliman, and T. Thonhauser, *J. Mater. Chem. A* **1**, 13597 (2013).
- [44] N. Nijem, P. Canepa, U. Kaipa, K. Tan, K. Roodenko, S. Tekarli, J. Halbert, I. W. H. Oswald, R. K. Arvapally, C. Yang, T. Thonhauser, M. A. Omary, and Y. J. Chabal, *J. Am. Chem. Soc.* **135**, 12615 (2013).
- [45] K. Tan, S. Zuluaga, Q. Gong, P. Canepa, H. Wang, J. Li, Y. J. Chabal, and T. Thonhauser, *Chem. Mater.* **26**, 6886 (2014).
- [46] S. Zuluaga, P. Canepa, K. Tan, Y. J. Chabal, and T. Thonhauser, *J. Phys. Condens. Matter* **26**, 133002 (2014).
- [47] V. A. Dediu, L. E. Hueso, I. Bergenti, and C. Taliani, *Nat. Mater.* **8**, 707 (2009).
- [48] M. Musiał and S. A. Kucharski, *J. Chem. Theory Comp.* **10**, 1200 (2014).
- [49] G. M. Sipahi, I. Zutic, N. Atodiresei, R. W. Kawakami, and P. Lazic, *J. Phys.: Condens. Matter* **26**, 104204 (2014).
- [50] O. Gunnarsson, B. I. Lundqvist, and J. W. Wilkins, *Phys. Rev. B* **10**, 1319 (1974).

- [51] The functionals VV09 [37] and VV10 [38], while related to vdW-DF, follow a different, simpler philosophy in defining the nonlocal correlation kernel. Spin does not affect the plasmon dispersion in VV09, and the VV09 strategy cannot be used for including spin in the vdW-DF method. Also note that no proper spin formulation exists for VV10 and the VV10 implementations use a spin-balancing procedure [53] to compute E_c^{nl} .
- [52] VV09 [37] is only implemented in the real-space code Q-Chem [90] and a direct comparison to svdW-DF results for periodic crystals such as MOFs is thus not possible.
- [53] Some DFT codes permit a pragmatic adaption of non-local functionals to spin systems, namely computing E_c^{nl} based on the total electron density, leaving $E_{xc}^0[n_\uparrow, n_\downarrow]$ to reflect all spin effects. This spin-balanced E_c^{nl} evaluation constitutes an uncontrolled approximation, ignoring that spin changes the plasmon dispersion.
- [54] E. Ziambaras, J. Kleis, E. Schröder, and P. Hyldgaard, Phys. Rev. B **76**, 155425 (2007).
- [55] M. Obata, M. Nakamura, I. Hamada, and T. Oda, J. Phys. Soc. Jpn. **82**, 093701 (2013).
- [56] M. Obata, M. Nakamura, I. Hamada, and T. Oda, (2015), <http://arxiv.org/abs/1501.05081>.
- [57] O. Gunnarsson and B. I. Lundqvist, Phys. Rev. B **13**, 4274 (1976).
- [58] U. von Barth and L. Hedin, J. Physics C: Solid State Phys. **5**, 1629 (1972).
- [59] R. O. Jones and O. Gunnarsson, Rev. Mod. Phys. **61**, 689 (1989).
- [60] Note that svdW-DF reduces to vdW-DF in the absence of spin polarization.
- [61] D. C. Langreth and J. P. Perdew, Phys. Rev. B **15**, 2884 (1977).
- [62] H. Rydberg, M. Dion, N. Jacobson, E. Schröder, P. Hyldgaard, S. I. Simak, D. C. Langreth, and B. I. Lundqvist, Phys. Rev. Lett. **91**, 126402 (2003).
- [63] J. P. Perdew and Y. Wang, Phys. Rev. B **33**, 8800 (1986).
- [64] G. D. Mahan, J. Chem. Phys. **43**, 1569 (1965).
- [65] K. Rapcewicz and N. W. Ashcroft, Phys. Rev. B **44**, 4032 (1991).
- [66] P. Giannozzi, S. Baroni, N. Bonini, M. Calandra, R. Car, C. Cavazzoni, D. Ceresoli, G. L. Chiarotti, M. Cococcioni, I. Dabo, A. Dal Corso, S. de Gironcoli, S. Fabris, G. Fratesi, R. Gebauer, U. Gerstmann, C. Gougoussis, A. Kokalj, M. Lazzeri, L. Martin-Samos, N. Marzari, F. Mauri, R. Mazzarello, S. Paolini, A. Pasquarello, L. Paulatto, C. Sbraccia, S. Scandolo, G. Sclauzero, A. P. Seitsonen, A. Smogunov, P. Umari, and R. M. Wentzcovitch, J. Phys. Condens. Matter **21**, 395502 (2009).
- [67] W. Zhou, H. Wu, and T. Yildirim, J. Am. Chem. Soc. **130**, 15268 (2008).
- [68] M. Märçz, R. E. Johnsen, P. D. Dietzel, and H. Fjellvåg, Micropor. Mesopor. Mat. **157**, 62 (2012).
- [69] D. Yu, A. O. Yazaydin, J. R. Lane, P. D. C. Dietzel, and R. Q. Snurr, Chem. Sci. **4**, 3544 (2013).
- [70] S. R. Caskey, A. G. Wong-Foy, and A. J. Matzger, J. Am. Chem. Soc. **130**, 10870 (2008).
- [71] P. D. C. Dietzel, V. Besikiotis, and R. Blom, J. Mater. Chem. **19**, 7362 (2009).
- [72] C. Linton, F. Martin, A. Ross, I. Russier, P. Crozet, A. Yiannopoulou, L. Li, and A. Lyyra, J. Mol. Spectrosc. **196**, 20 (1999).
- [73] J. A. Pople, M. Head-Gordon, D. J. Fox, K. Raghavachari, and L. A. Curtiss, J. Chem. Phys. **90**, 5622 (1989).
- [74] Y. Gamo, A. Nagashima, M. Wakabayashi, M. Terai, and C. Oshima, Surf. Sci. **374**, 61 (1997).
- [75] A. Varykhalov, J. Sánchez-Barriga, A. M. Shikin, C. Biswas, E. Vescovo, A. Rybkin, D. Marchenko, and O. Rader, Phys. Rev. Lett. **101**, 157601 (2008).
- [76] Y. S. Dedkov and M. Fonin, New J. Phys. **12**, 125004 (2010).
- [77] P. Canepa, Y. J. Chabal, and T. Thonhauser, Phys. Rev. B **87**, 094407 (2013).
- [78] L. Wang, T. Maxisch, and G. Ceder, Phys. Rev. B **73**, 195107 (2006).
- [79] E. D. Bloch, L. J. Murray, W. L. Queen, S. Chavan, S. N. Maximoff, J. P. Bigi, R. Krishna, V. K. Peterson, F. Grandjean, G. J. Long, B. Smit, S. Bordiga, C. M. Brown, and J. R. Long, J. Am. Chem. Soc. **133**, 14814 (2011).
- [80] R. F. W. Bader, *Atoms in Molecules: A Quantum Theory* (Oxford University Press, New York, 1990).
- [81] G. Henkelman, A. Arnaldsson, and H. Jónsson, Comp. Mater. Science **36**, 354 (2006).
- [82] R. Sabatini, T. Gorni, and S. de Gironcoli, Phys. Rev. B **87**, 041108(R) (2013).
- [83] K. F. Garrity, J. W. Bennett, K. M. Rabe, and D. Vanderbilt, Comp. Mat. Science **81**, 446 (2014).
- [84] Caution must be used when using DFT to determine the Li dimer triplet binding. We find that all tested local, semilocal, and nonlocal spin-density functionals underestimate the experimental binding separation of 4.2 Å [72] by 0.5 – 0.7 Å, with svdW-DF-cx and LDA giving the smallest and largest deviation, respectively.
- [85] D. D. Konowalow and J. L. Fish, Chem. Phys. **84**, 463 (1984).
- [86] R. Poteau and F. Spiegelmann, J. Mol. Spect. **171**, 299 (1995).
- [87] P. Jasik and J. E. Sienkiewicz, Chem. Phys. **323**, 563 (2006).
- [88] J. C. Grossman, J. Chem. Phys. **117**, 1434 (2002).
- [89] M. W. Chase, NIST-JANAF Thermochemical Tables, 4th ed., J. Phys. Chem. Ref. Data Monogr. **9**, Suppl. 1 (1998).
- [90] Y. Shao, L. F. Molnar, Y. Jung, J. Kussmann, C. Ochsenfeld, S. T. Brown, A. T. Gilbert, L. V. Slipchenko, S. V. Levchenko, D. P. O'Neill, R. A. DiStasio Jr, R. C. Lochan, T. Wang, G. J. Beran, N. A. Besley, J. M. Herbert, C. Yeh Lin, T. Van Voorhis, S. Hung Chien, A. Sodt, R. P. Steele, V. A. Rassolov, P. E. Maslen, P. P. Korambath, R. D. Adamson, B. Austin, J. Baker, E. F. C. Byrd, H. Dachsel, R. J. Doerksen, A. Dreuw, B. D. Dunietz, A. D. Dutoi, T. R. Furlani, S. R. Gwaltney, A. Heyden, S. Hirata, C.-P. Hsu, G. Kedziora, R. Z. Khalliulin, P. Klunzinger, A. M. Lee, M. S. Lee, W. Liang, I. Lotan, N. Nair, B. Peters, E. I. Proynov, P. A. Pieniazek, Y. Min Rhee, J. Ritchie, E. Rosta, C. David Sherrill, A. C. Simmonett, J. E. Subotnik, H. Lee Woodcock III, W. Zhang, A. T. Bell, A. K. Chakraborty, D. M. Chipman, F. J. Keil, A. Warshel, W. J. Hehre, H. F. Schaefer III, J. Kong, A. I. Krylov, P. M. W. Gill, and M. Head-Gordon, Phys. Chem. Chem. Phys. **8**, 3172 (2006).